

# Optical Engineering

OpticalEngineering.SPIEDigitalLibrary.org

## **Rec.2100 color gamut revelation using spectrally ultranarrow emitters**

Sinan Genc  
Mustafa Uguz  
Osman Yilmaz  
Evren Mutlugun

**SPIE.**

Sinan Genc, Mustafa Uguz, Osman Yilmaz, Evren Mutlugun, "Rec.2100 color gamut revelation using spectrally ultranarrow emitters," *Opt. Eng.* **56**(11), 115106 (2017), doi: 10.1117/1.OE.56.11.115106.

# Rec.2100 color gamut revelation using spectrally ultranarrow emitters

Sinan Genc,<sup>a</sup> Mustafa Uguz,<sup>b</sup> Osman Yilmaz,<sup>b</sup> and Evren Mutlugun<sup>a,\*</sup>

<sup>a</sup>Abdullah Gül University, Faculty of Engineering, Department of Electrical and Electronics, Sumer Campus, Kayseri, Turkey

<sup>b</sup>Arcelik A.S., Beylikduzu, Istanbul, Turkey

**Abstract.** We theoretically simulate the performance of ultranarrow emitters for the first time to achieve record high coverage for the International Telecommunication Union Radiocommunication Sector BT.2100 (Rec.2100) and National Television System Committee (NTSC) color gamut. Our results, employing more than 130-m parameter sets, include the investigation into peak emission wavelength and full width at half maximum (FWHM) values for three primaries that show ultranarrow emitters, i.e., nanoplatelets are potentially promising materials to fully cover the Rec.2100 color gamut. Using ultranarrow emitters having FWHM as low as 6 nm can provide the ability to attain 99.7% coverage area of the Rec.2100 color gamut as well as increasing the NTSC triangle to 133.7% with full coverage. The parameter set that provides possibility to fully reach Rec.2100 also has been shown to match with D65 white light by making use of the correct combination of those three primaries. Furthermore, we investigate the effect of the fourth color component on the CIE 1931 color space without sacrificing the achieved coverage percentages. The investigation into the fourth color component, cyan, is shown for the first time to enhance the Rec.2100 gamut area to 127.7% with 99.9% coverage. The fourth color component also provides an NTSC coverage ratio of 171.5%. The investigation into the potential of emitters with ultranarrow emission bandwidth holds great promise for future display applications. © 2017 Society of Photo-Optical Instrumentation Engineers (SPIE) [DOI: [10.1117/1.OE.56.11.115106](https://doi.org/10.1117/1.OE.56.11.115106)]

Keywords: quantum dot; nanoplatelet; display; color gamut; white light.

Paper 171244 received Aug. 8, 2017; accepted for publication Oct. 31, 2017; published online Nov. 22, 2017.

## 1 Introduction

Backlight systems for display technology had a great development from cold cathode fluorescent lamps that have 65% to 70% of NTSC color gamut to light-emitting diodes (LEDs) have ~96% of NTSC triangle on CIE 1931. LEDs provided a better visualization along with a reasonable cost compared with the previous illuminants.<sup>1,2</sup> Achieving appropriate color quality for a backlight unit has been an important figure of merit for a display in terms of compatibility between the proposed system and television technology. Increasing the color gamut, which means increasing the existing colors on displays among all the colors that can be perceived by the human eye, would provide more real colors on displays, and LEDs have given proper results for the first step as backlight and the quality of displays increased dramatically.<sup>3,4</sup>

In the beginning stages of LED backlight technology, RGB LEDs were used and the color gamut was ~105% of NTSC.<sup>5</sup> The performance was greater than the technology of that era in terms of color quality but complex driving circuits and high-energy consumption directed the industry to the use of white LEDs using color converters. Although the cost has been decreased, broad emission of white LEDs caused a regression in color quality. The gamut ratio was ~70%.<sup>5</sup> To enhance the backlight systems in terms of color quality, cost, and energy saving, the quantum dots (QDs) have started to arise as new backlight units.<sup>6–8</sup> Its narrow

emission spectra, high photoluminescence efficiency, and ease in controllability of optical properties described them as both an efficient and meaningful choice.<sup>9,10</sup>

The announcement of ITU-R BT.2100 (Rec.2100) has increased the need in terms of color quality.<sup>11</sup> A wider color gamut than HDTV—that means a broader gamut than sRGB—has identified in Rec. 2100. Table 1 indicates the chromaticity coordinates for the red (R), green (G), and blue (B) primaries, the reference white point, and the appropriate peak emission wavelengths, respectively.

Achieving the new wider color triangle requires purer colors that mean narrower emissions on appropriate emission wavelengths. On the one hand, monochromatic light sources, such as lasers, may compensate that necessity but that technology may be available in the near future.<sup>12</sup> On the other hand, QDs having FWHM between 30 and 60 nm are not able to balance that lack.<sup>13</sup> At that point, the need of a backlight system that provides a wider gamut and efficiency in terms of cost has occurred. Ultranarrow emitters are effective in terms of both performance and cost as new backlight units to ultrahigh-definition television technology, and they can also support today's technology in terms of NTSC color gamut.

Ultranarrow emitters have narrower emission spectra than QDs such as <10 nm, which can be an alternative way to achieve the Rec.2100 color gamut. For instance, using CdSe nanoplatelets can open a new window to both achieve and enhance the color gamut of Rec.2100. They have emission width approximately from 7 to 8 nm to 12 nm.<sup>14</sup>

\*Address all correspondence to: Evren Mutlugun, E-mail: [evren.mutlugun@agu.edu.tr](mailto:evren.mutlugun@agu.edu.tr)

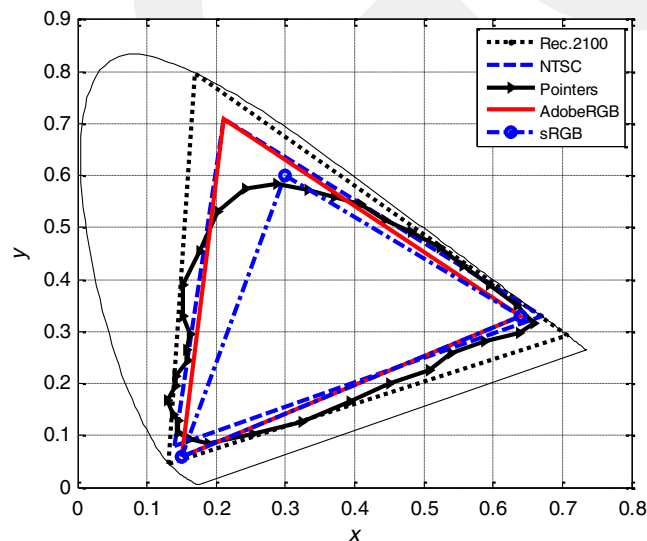
**Table 1** Defined colorimetric data at ITU-R BT.2100 (Rec.2100).

Primaries and white point	x coordinate on CIE 1931	y coordinate on CIE 1931	Corresponding wavelength
R	0.708	0.292	630 nm
G	0.170	0.797	532 nm
B	0.131	0.046	467 nm
White	0.313	0.329	D65 (Illuminant)

The comparison of Rec.2100 color gamut with other color standards such as Rec.709 (sRGB),<sup>15</sup> NTSC,<sup>16</sup> Adobe RGB,<sup>17</sup> and Pointer's colors<sup>18</sup> has shown in Fig. 1. As can be seen, the area of Rec.2100 covers sRGB, Adobe RGB and it intersects with areas of NTSC and Pointer's Gamut >99%. The figure also indicates that Rec.2100 almost covers all other standards used before, and it has all of its corners just on the border of spectral locus. In future, the new development will be most probably on green corner because of the existence of wide area compared with the other corners to cover and the "green gap" issue, but that improvement will cause some missing coordinates covered in Rec.2100 due to having corners on spectral locus.

One important point is the meaning of increment on color gamut ratio. The "area ratio" is the ratio between triangular area of the proposed primaries and the standard RGB triangular area ( $A_{\text{proposed}}/A_{\text{standard}}$ ), such as sRGB or NTSC. In the "coverage ratio," the numerator is the intersecting area between standard triangle and proposed triangle ( $A_{\text{proposed}} \cap A_{\text{standard}}/A_{\text{standard}}$ ).<sup>19</sup> It is clear that the latter is preferable so that in this study all percentages refer to coverage ratio, which means the intersecting areas between the referenced color gamut and the preferred color gamut.

The other key point is the selection of color space. Although CIE 1931 color space is the most commonly used one, the nonuniformity is the main disadvantage for that

**Fig. 1** Rec.2100, NTSC, Pointers, AdobeRGB, and sRGB reference color gamuts on CIE 1931 color space.

color space. The distance between different color positions on CIE 1931 is not the same as that perceived by the human eye. The other color spaces, i.e., CIE 1976, CIECAM02, and CIELAB exist in the literature to provide better uniformity using two or three dimensions.<sup>19–22</sup> In this study, CIE 1931 color space has been used instead of CIE 1976 as a result of having more consistent relation with other color spaces and more opportunity to compare with the previous studies in the literature.

In this study, first, we investigate the performance of emitters including both narrow emitters i.e., QDs and ultranarrow emitters, i.e., nanoplatelets to be able to achieve Rec.2100 color gamut. We obtain the results that (1) it is not possible to have the whole area of Rec.2100 using green emitter, which have FWHM higher than 15 nm because of not enough emission narrowness, (2) using ultranarrow emitters such as the Rec.2100 area is almost achievable, (3) the emission wavelengths for widest coverage area are around the corresponding wavelengths announced in Rec.2100 except from the red emitter due to the nonuniformity of color space, and (4) a new enhancement in future will cause a loss from the coordinates covered in Rec.2100.

## 2 Determination of Parameters

Defining appropriate parameters of FWHM and emission wavelength to enhance the gamut is the key point of that step. Using corresponding emission wavelengths declared in Rec. 2100 with an extra range from both left and right sides with the aim to not miss any proper result would be logical in terms of identifying emission wavelengths. For FWHM side, most of the research done in that area has specified that QDs can reach to 30-nm range for red and green components. For a structure that used blue LED and red and green QD layers to get white light, the FWHM of blue LED can be chosen as 20 to 30 nm.<sup>8</sup> Regarding the FWHM ranges of ultranarrow emitters, the limits of emission width can be defined from 6 to 30 nm. Therefore, the ranges for simulation are defined as 451 to 475 nm, 514 to 540 nm, and 610 to 700 nm for blue, green, and red emission wavelengths, respectively. FWHM variables for all three primaries are between 6 and 30 nm. The increments in the emission wavelength and FWHM are 2 and 1 nm, respectively.

In Fig. 2, the colored areas include all possibilities for the coordinates of all primaries. The emission wavelength and FWHM parameters chosen result in values on those areas. Not all but most of the coordinates exist in those areas are appropriate to achieve Rec.2100 gamut.

To use the emission wavelength and FWHM parameters for white, the intensities of three primaries also have to be considered. After determination of the first two parameters, emission wavelength and FWHM, the percentages of the white will be considered using those emission wavelength and FWHM parameters. The intensity percentages are defined with a sensibility of 1%.

## 3 Simulation

In the simulation part, in MATLAB, we used the ranges determined above. The Gauss distribution was referenced for the emissions, which have at least 20-nm FWHM, and for the others, Lorentzian distribution was defined because the spectra of emitters at those FWHM levels, such as nanoplatelets, fit Lorentzian better.

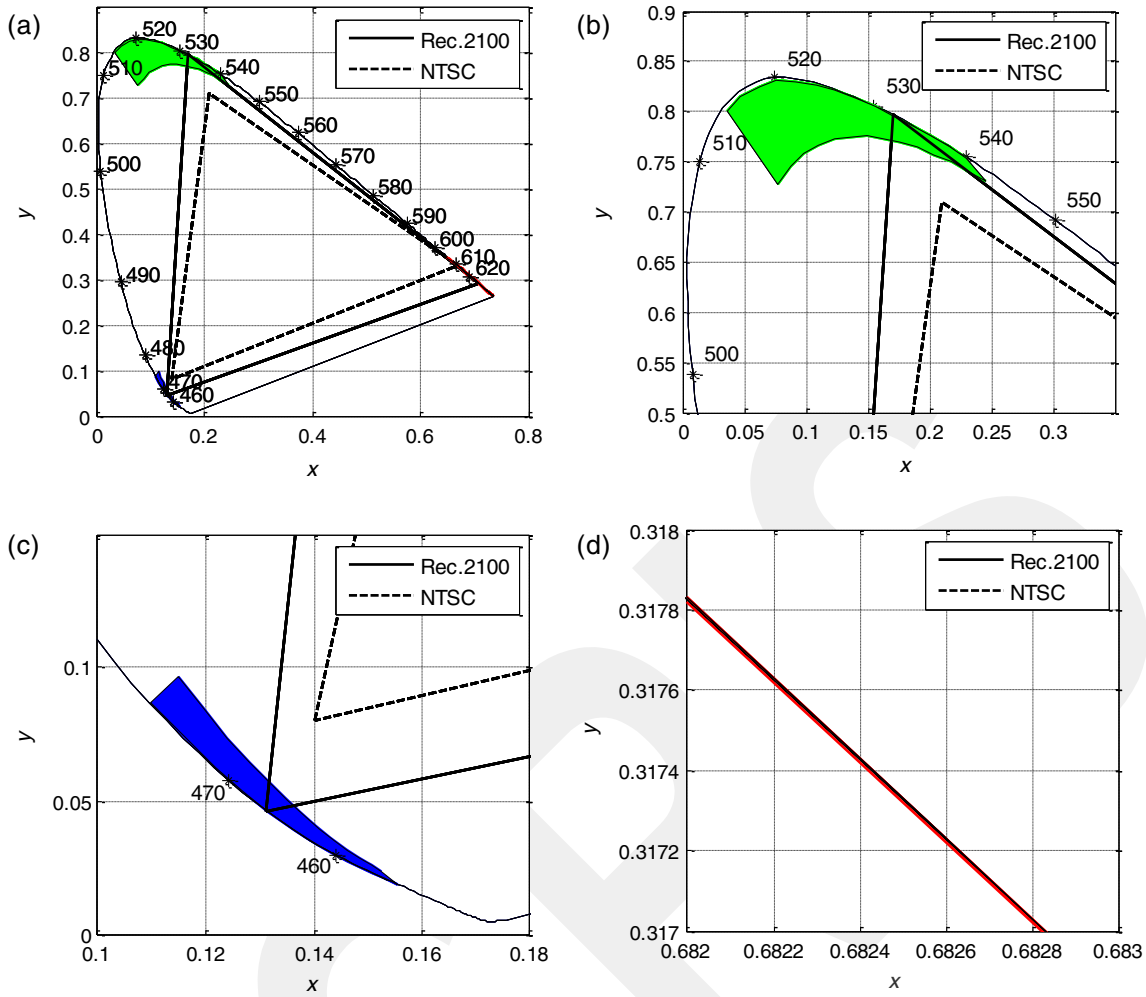


**Fig. 2** On CIE 1931, (a) NTSC and Rec.2100 reference triangles with highlighted zones of three color primaries, (b) simulation zone of green component, (c) blue simulation zone, and (d) simulation zone of red primary.

In simulation step, using *nested for loops* all color parameters at all defined ranges have been taken into consideration and input sets, which include peak emission wavelength and FWHM for each emitter were defined. Calculation of tristimulus values of each data set was the next step of the simulation and for a spectral power distribution of  $s(\lambda)$ , Eqs. (1)–(3) given below, have been used for blue, green, and red tristimulus values, respectively

$$X = \int_{\lambda} s(\lambda) \bar{x}(\lambda) d\lambda, \tag{1}$$

$$Y = \int_{\lambda} s(\lambda) \bar{y}(\lambda) d\lambda, \tag{2}$$

$$Z = \int_{\lambda} s(\lambda) \bar{z}(\lambda) d\lambda, \tag{3}$$

where  $\bar{x}(\lambda)$ ,  $\bar{y}(\lambda)$ , and  $\bar{z}(\lambda)$  are the color matching functions of CIE 1931 2-deg standard color observer.

Chromaticity coordinates of all red, green, and blue emitters were calculated with these tristimulus values as

$$x = \frac{X}{X + Y + Z}, \tag{4}$$

$$y = \frac{Y}{X + Y + Z}. \tag{5}$$

At least, having all three chromaticity coordinates for primaries and considering Rec. 2100 and NTSC color gamut corner coordinates provided comparison between simulated and referenced color gamuts. We got >130 million (130, 312, and 500) results that include parameters of FWHM and emission wavelength, white, red, green, and blue coordinates, coverage percentages of Rec.2100 and NTSC.

As a result, the best coverage percentage of Rec.2100 is 99.7%. The color parameters for red, green, and blue are 632, 532, and 467 nm for emission wavelengths and 11, 6, and 7 nm for FWHM values, respectively. Those parameters broaden the NTSC color triangle 133.7% with a coverage ratio of >99.9% as can be seen in Fig. 3 and they cover other color standards, such as Adobe RGB and sRGB.

From the viewpoint of peak emission wavelengths, the results are almost the same with corresponding peak emission wavelength announced in the Rec.2100 standards.

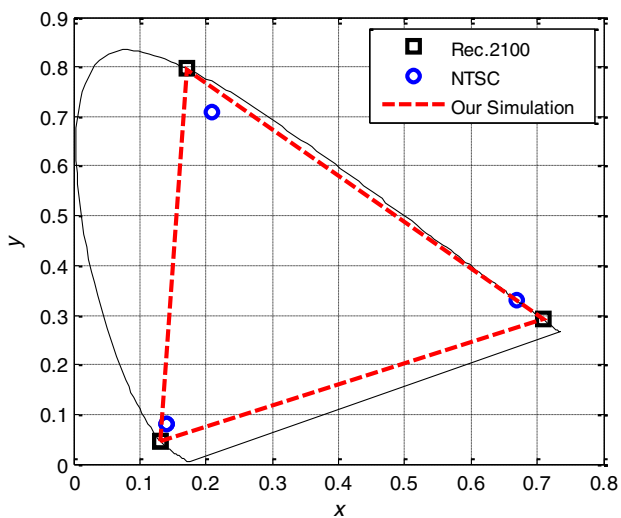


Fig. 3 Corner coordinates of Rec.2100 and NTSC color references along with our highest area simulation result.

In Fig. 4, the data sets providing >99% Rec.2100 coverage have been given. As it indicates, up to 30-nm FWHM for blue emitter is appropriate around the corresponding wavelength, which is in the range of 465 to 469 nm. The green emitter is the one that is most critically important to cover Rec.2100. Only 530- and 532-nm peak emission wavelengths are proper to use and up to the widest 13-nm FWHM can provide the coverage of Rec.2100. Finally, the red portion is the most flexible zone to cover Rec.2100. The nonuniformity gives the chance to use a broadband red emission spectrum in that part. It is possible to obtain higher Rec.2100 coverage levels starting from 628- to 700-nm peak emission wavelength and from 6- to 30-nm FWHM value as shown in Fig. 4.

The results were separated on MATLAB considering coverage ratio of Rec.2100 and shown in Table 2. Having most of the results in such higher percentages proves that the peak emission wavelength and FWHM parameters have been defined properly.

In Table 3, the coordinates of primaries in Rec.2100 and optimum simulation result are given. The differences between Rec.2100 coordinates and proposed coordinates

Table 2 Distribution of coverage ratio on Rec.2100.

Coverage ratio (C.R.)	Number of data sets	Percentage of data sets (%)
C.R. $\geq 99\%$	219,697	<1
99% > C.R. $\geq 95\%$	24,945,483	19
95% > C.R. $\geq 90\%$	48,826,342	37
90% > C.R. $\geq 80\%$	53,778,719	41
80% > C.R. $\geq 70\%$	2,537,438	2

arise from the sensibility of defined peak emission wavelength and FWHM parameters. If 2 nm for emission wavelength and 1 nm for FWHM are shrunk to <1-nm increments, the difference would disappear.

In the new color gamut, a reference white coordinate must be chosen and the D65 seems as the best one. As it is indicated in Rec. 2100, because of the appropriation of the new system to the current technology, the D65 white coordinate has been referenced. Arranging the intensity values of red, green, and blue color primaries, that coordinate can be achieved. Increments of 1 nm have been arranged for intensity loops and all possibilities have been checked to obtain D65 white coordinate.

Correlated color temperature (CCT) gives information about the temperature of color referencing of the Planckian Blackbody radiator and the closest distance from the coordinate of the color to it. The Robertson method is commonly

Table 3 Chromaticity coordinates of three primaries in Rec.2100 and optimum simulation result.

Coordinate in Rec.2100	Coordinate in simulation
(0.131, 0.046)	(0.131, 0.047)
(0.170, 0.797)	(0.171, 0.796)
(0.708, 0.292)	(0.709, 0.291)

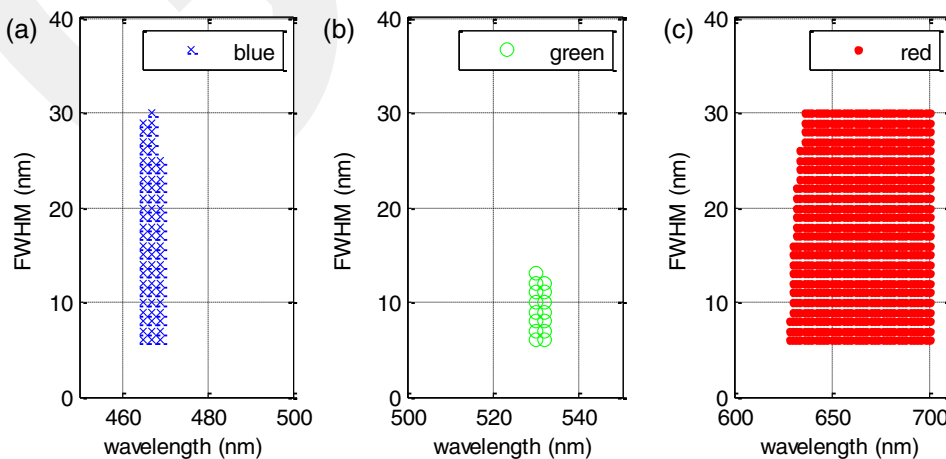


Fig. 4 The relation between peak emission wavelength and FWHM for data sets giving <99% Rec.2100 coverage for (a) blue, (b) green, and (c) red emitters.

**Table 4** Distribution of CCT (4000 ≤ CCT ≤ 10,000) in simulation results.

CCT range (°K)	Number of data sets
CCT ≤ 4000	859
5000 ≥ CCT > 4000	280
6000 ≥ CCT > 5000	311
7000 ≥ CCT > 6000	357
10,000 ≥ CCT > 7000	755

used for that calculation.<sup>23</sup> D65 illuminant has a CCT 6500 K. The simulation for CCT parameters and D65 white has been run using corresponding peak emission wavelengths that gave the best coverage ratio. Peak emission wavelengths of 467, 532, and 632 nm and FWHM values of 7, 6, and 11 nm have been used for blue, green, and red emitters, respectively. In 4851 datasets with 1-nm increment of intensity steps in the simulation, as can be seen in Table 4, 357 data sets, which give the CCT parameter around 6500 K, are presented which belong to the D65 white.

In Fig. 5(a), using defined peak emission wavelengths and FWHM parameters, all different intensity possibilities are simulated for the CCT. It seems that the green component has its top value around 7500 K and after that it starts to decrease. The blue intensity can have all possibilities under 50% until 7500 K, and then its percentage increases through higher temperatures. The red intensity has a sharp decrease until 7500 K again. In Fig. 5(b), the range between 6000 and 7000 K, which includes the D65 white coordinate, is focused, and it is seen that the green component is dominant for that range.

The illuminant D65 has coordinates (0.3128, 0.3290) and in our results, we check white around that reference using 0.3028 to 0.3228 for  $x$ -coordinate and 0.3190 to 0.3390 for  $y$ -coordinate. Among all intensity possibilities, 10 intensity

sets are eligible. Those sets are visualized in Fig. 6(a) and focused in Fig. 6(b) using defined emission wavelength and FWHM sets. The intensity percentages of the sets used in the area investigated are shown in Fig. 7.

As can be seen from Fig. 7, the blue intensity percentage changes between 30% and 33%. The green intensity can change from 34% to 37% and finally red has a range between 31% and 34%. Additionally, the optimum parameter set that provides the closest white coordinate to the D65 with <0.005 unit distance is 32%, -36%, and -32% for blue, green, and red, respectively. Using 1-nm increment in the intensity level, we achieve  $(x:y)$  of (0.3140:0.3254), which is close to D65 white coordinates (0.3128:0.3290). Decreasing the step size to <1% intensity increment in simulation provides more sensible results to achieve the exact coordinate of D65.

The addition of color filters to the simulation system is the next step of this study. In Fig. 8(a), transmission spectra of commercial RGB color filters are shown and in Fig. 8(b), the white light that gives highest color gamut and closest white coordinate to D65 is shown with its filtered version. The Rec.2100 coverage ratio is 87.2% after filter application. From the viewpoint of NTSC, the ratio is 116.8% with 99.4% coverage. Increasing those values is possible by redesigning and decreasing the crosstalk between transmission spectra of color filters.

Having a wider area on CIE can be achieved using a fourth color component. The fourth component, cyan, can support both enhancement of the area and coverage of the Rec.2100. Sharp Electronics, the television producer, announced a four-color television technology, Quattron, in 2010.<sup>24,25</sup> They stated that the fourth component, yellow, increases the color range and brightness, and it also lowers the energy consumption. Starting from this point, to increase the color range more, we add cyan as a fourth component. The main reason for choosing cyan is the resolution limit of the human eye. Just noticeable difference is experimentally found to be 0.01 in CIE 1931 color space for red and white, 0.02 for green, and <0.005 for blue region.<sup>26</sup> The use of cyan as the fourth color component will provide a large scale of

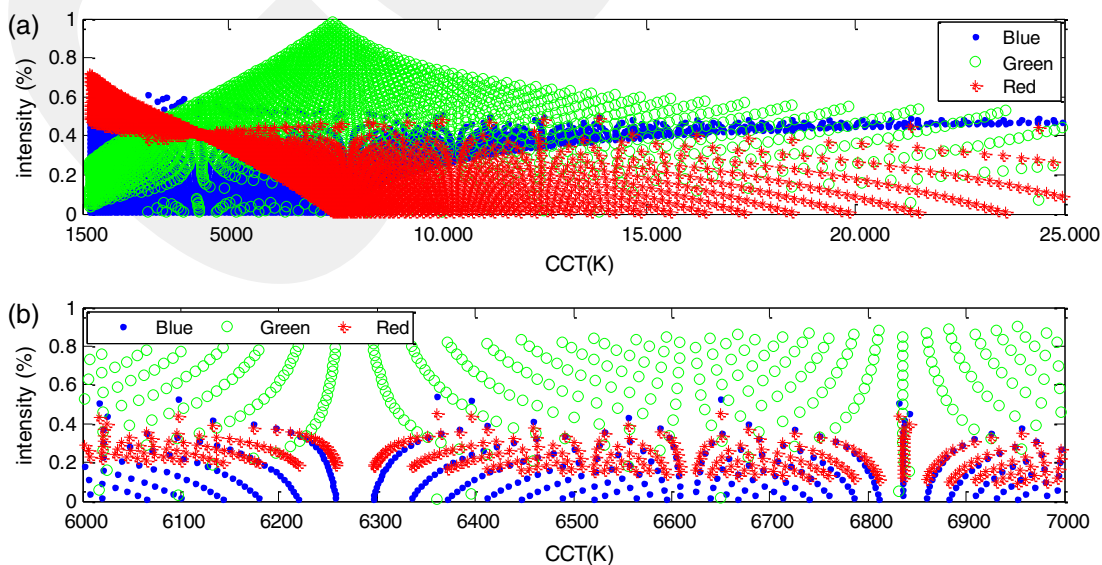


**Fig. 5** (a) The distribution of intensities of three primaries between (a) 1500 and 25,000 K (b) 6000 to 7000 K, which is around the CCT D65.

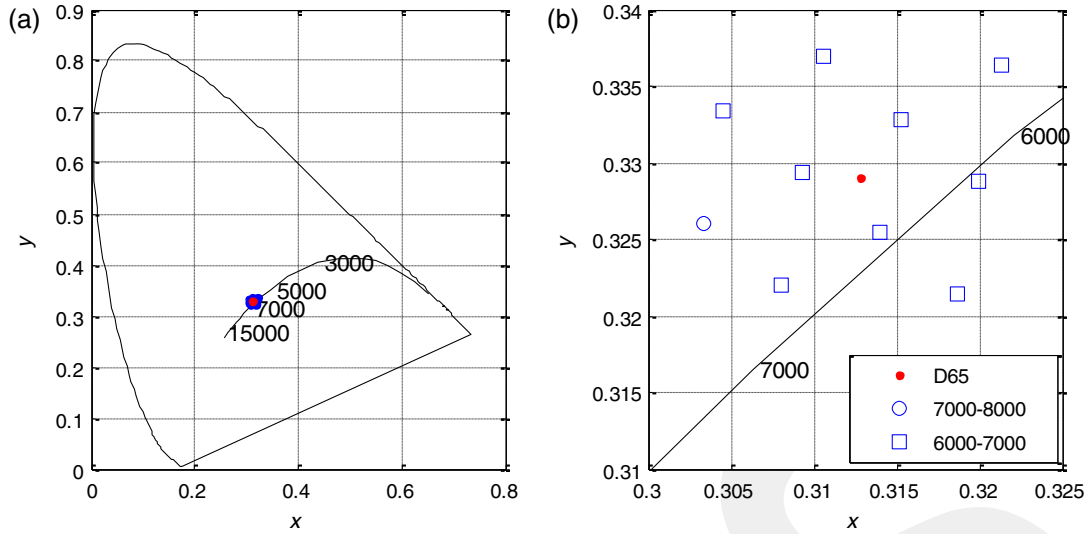


**Fig. 6** (a) The representation of the coordinates has a CCT between 6000—and 7000 K and (b) the coordinates in proximity of D65 coordinate, which is (0.3128, 0.3290) for x- and y-axis.

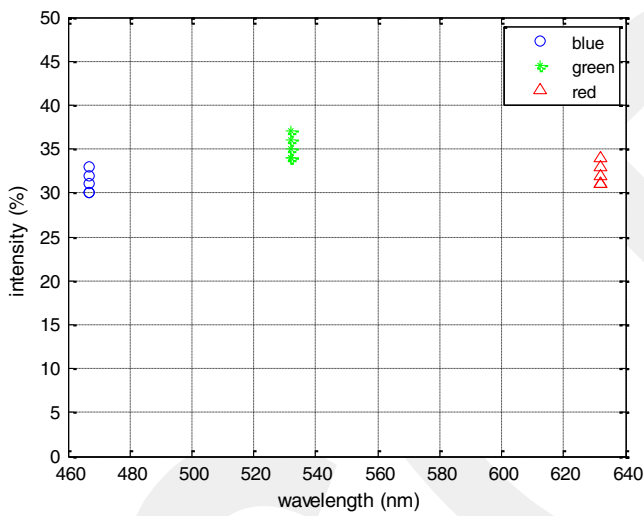


**Fig. 7** Intensity values of three primary colors.

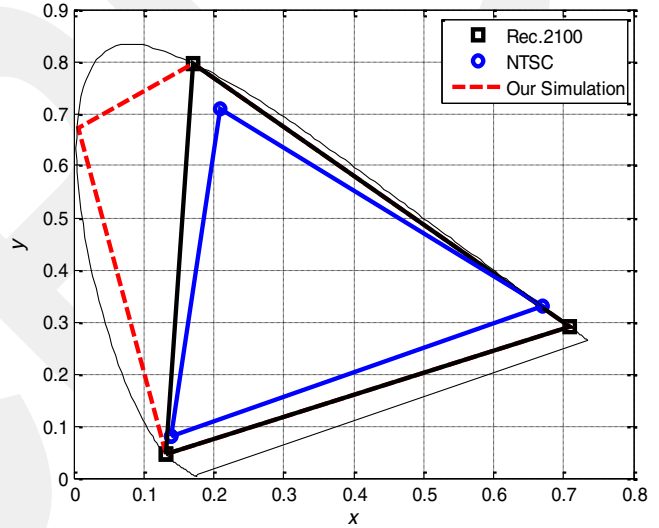


**Fig. 9** Color gamuts of Rec.2100, NTSC and our four-color simulation on CIE 1931.

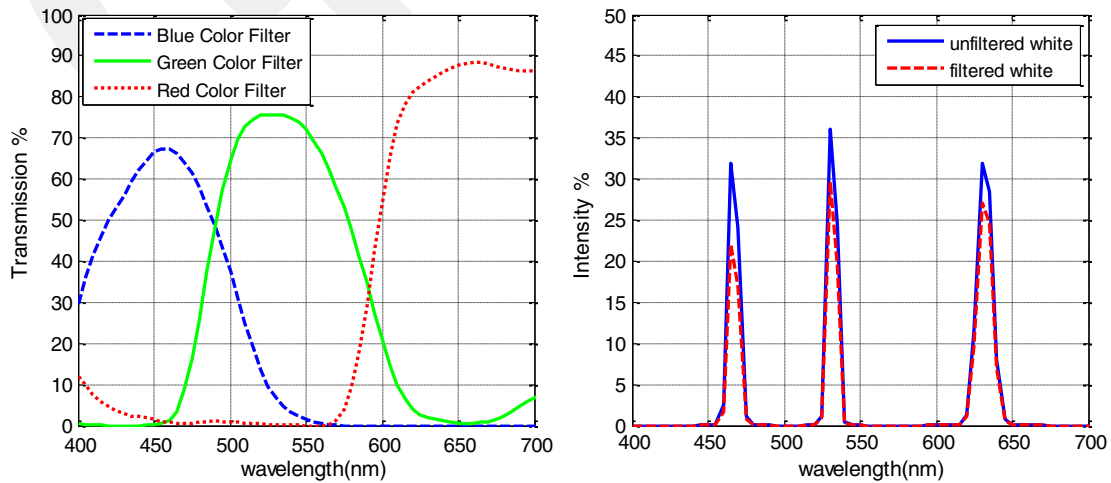


**Fig. 8** (a) Transmission spectra of commercial RGB color filters and (b) filtered and unfiltered spectra of white light.

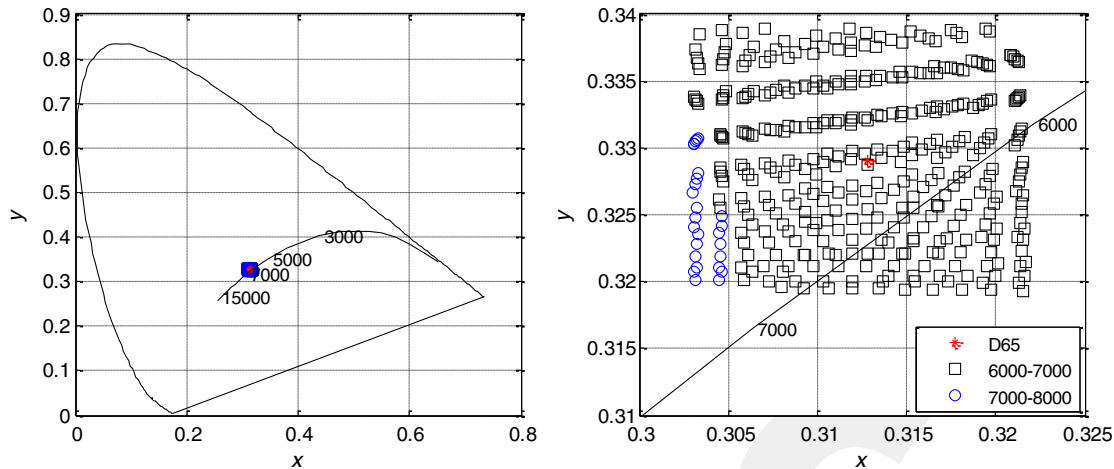


**Fig. 10** (a) The coordinates closest to the D65 in four-color mixture and (b) closest white coordinates to D65 reference classified according to the CCT values between 6000 and 8000 K.

different colors as an addition to the achieved color gamut. We achieved 127.70% of Rec.2100 color triangle with a minor sacrifice, which is 0.13% using 506 nm for peak emission wavelength and 6 nm for FWHM as emission parameters. The coverage situation of Rec.2100 for four component simulation can be seen in Fig. 9. The same parameter set also increases the value of NTSC enhancement up to 171.03% with 99.98% coverage and the percentage of achieved colors on CIE is 80.93. We believe that our study will be a supplementary documentation for the literature.

In Fig. 10(a), the 375 sets closer to the D65 are visualized and in Fig. 10(b), they are zoomed and classified considering CCT value. The intensity percentages that belong to the 375 closest data sets to D65 are shown in Fig. 11. For a closer coordinate to reference white, the blue intensity percentage can vary from 15% to 33%. The red intensity range can be between 27% and 34%. The green may change from 1% to 37% and the fourth component cyan, can change from 1% up to 56% as can be understood from Fig. 11. Having such wide cyan intensity range provides many data set opportunities to get reference white in terms of arranging intensities of emitters.

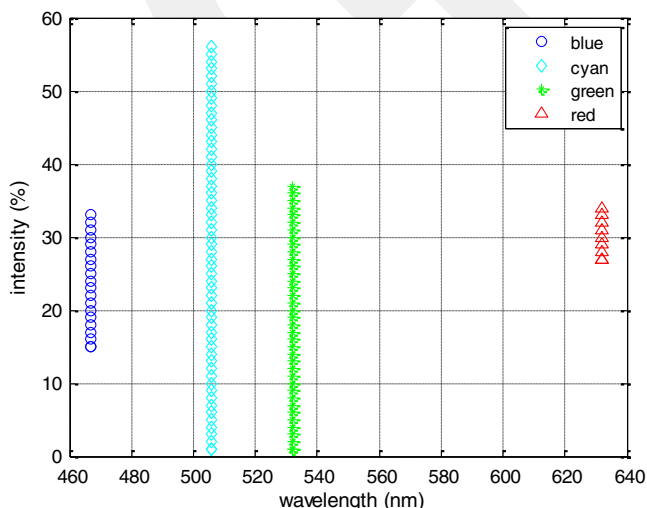


**Fig. 11** The intensities of primaries including the cyan component.

The closest one among those 375 sets to D65 white have intensity percentages for blue, cyan, green, and red are 19%, 45%, 7%, and 29%, respectively.

#### 4 Conclusion

In >130 million results, it is clear that using green emitter having FWHM higher than 15 nm is not an appropriate way to enlarge, or even to achieve the Rec.2100 due to the thickness of emission. The ultranarrow emitters, have FWHM about 6 to 7 nm, can be the new focusing area in terms of color performance. Use of ultranarrow emitters, i.e., nanoplatelets as backlight sources, can open a new window to display technology. However, corresponding wavelengths declared in Rec.2100 have been used to deduce these results about emission bandwidth. Only in red region, as a result of nonuniformity, broad emission parameters, 628- to 700-nm peak emission wavelength, and 6- to 30-nm FWHM can provide the desired results.

In this study, we analyzed if it is possible to reach Rec.2100, which covers the NTSC triangle that is being used as an industrial standard, by ultranarrow emitters. Changing the reference from NTSC to Rec.2100 in industry may take time so the NTSC coverage with those results is quite important. We achieved a covered NTSC triangle with 133.7% increment, which is the highest coverage ratio announced up to now. The parameters to achieve that percentage also support covering 99.7% of Rec.2100. Another key point of the study is that the parameters are proper to adjust them for reference illuminant D65 so that the proposed parameters are appropriate to use for production.

In addition, we simulated a fourth component to investigate the coverage of Rec.2100 considering the NTSC enhancement and maximum achieved color percentage on CIE 1931. The fourth component, cyan, has the potential to increase the achieved color range up to 127.7% of Rec.2100 color gamut with 99.8% coverage by 506-nm peak emission wavelength and 6-nm FWHM values. The same sensibility range to achieve D65 (0.3028–0.3228 for  $x$ -coordinate and 0.3190 to 0.3390 for  $y$ -coordinate) includes 333 data sets for four color mixing.

## Acknowledgments

The authors would like to express thanks for financial support from the Scientific and Technological Research Council of Turkey TUBITAK under Project No. 5140079. E.M. acknowledges BAGEP 2014 Award.

## References

- R. J. Xie, N. Hirosaki, and T. Takeda, "Wide color gamut backlight for liquid crystal displays using three-band phosphor-converted white light-emitting diodes," *Appl. Phys. Express* **2**(2), 022401 (2009).
- K. Yoshimura et al., "White LEDs using the sharp  $\beta$ -sialon:Eu phosphor and Mn-doped red phosphorus for wide-color gamut display applications," *J. Soc. Inf. Disp.* **24**(7), 449–453 (2016).
- K. Kakinuma, "Technology of wide color gamut backlight with light-emitting-diode for liquid crystal display television," *Jpn. J. Appl. Phys.* **45**(5B), 4330–4334 (2006).
- T. Erdem and H. V. Demir, "Color science of nanocrystal quantum dots for lighting and displays," *Nanophotonics* **2**(1), 57–81 (2012).
- J. Chen et al., "A high-efficiency wide-color-gamut solid-state backlight system for LCDs using quantum dot enhancement film," in *SID Symp. Digest of Technical Papers*, Vol. 43, pp. 895–896 (2012).
- Z. Luo, Y. Chen, and S.T. Wu, "Wide color gamut LCD with a quantum dot backlight," *Opt. Express* **21**(22), 26269–26284 (2013).
- S. H. Lee et al., "Remote-type, high-color gamut white light-emitting based on InP quantum dot color converters," *Opt. Mater. Express* **4**(7), 1297–1302 (2014).
- J. S. Steckel et al., "Quantum dots: the ultimate down-conversion material for LCD displays," *J. Soc. Inf. Disp.* **23**(7), 294–305 (2015).
- Z. Luo, D. Xu, and S.T. Wu, "Emerging quantum-dots-enhanced LCDs," *J. Disp. Technol.* **10**(7), 526–539 (2014).
- S. Kim, S. H. Im, and S. W. Kim, "Performance of light-emitting-diode based on quantum dots," *Nanoscale* **5**, 5205–5214 (2013).
- ITU-R Recommendation BT.2100-1, "Image parameter values for high dynamic range television for use in production and international programme exchange," (2016).
- K. Masaoka, Y. Nishida, and M. Sugawara, "Designing display primaries with currently available light sources for UHDTV wide-gamut system colorimetry," *Opt. Express* **22**(16), 19069–19077 (2014).
- R. Zhu et al., "Realizing Rec.2020 color gamut quantum dot displays," *Opt. Express* **23**(18), 23680–23693 (2015).
- S. Ithurria, G. Bousquet, and B. Dubertret, "Continuous transition from 3D to 1D confinement observed during the formation of CdSe nanoplatelets," *J. Am. Chem. Soc.* **133**(9), 3070–3077 (2011).
- ITU-R Recommendation BT.709-5, "Parameter values for HDTV standards for production and international programme exchange," (2002).
- National Television System Committee, "Report and reports of panels," (1953).
- Adobe Systems Inc., "Adobe RGB (1998) color image encoding," (2005).
- M. R. Pointer, "The gamut of real surface colour," *Color Res. Appl.* **5**(3), 145–155 (1980).
- K. Masaoka and Y. Nishida, "Metric of color-space coverage for wide-gamut displays," *Opt. Express* **23**(6), 7802–7808 (2015).
- K. Masaoka, "Display gamut metrology using chromaticity diagram," *IEEE Access* **4**(16), 3878–3886 (2016).
- S. Wen, "A method for selecting display primaries to match a target color gamut," *J. Soc. Inf. Disp.* **15**(12), 1015–1022 (2007).
- K. Masaoka et al., "Design of primaries for a wide-gamut television colorimetry," *IEEE Trans. Broadcast.* **56**(4), 452–457 (2010).
- A. R. Robertson, "Computation of correlated color temperature and distribution temperature," *J. Opt. Soc. Am.* **58**(11), 1528–1535 (1968).
- SHARP, "Breathtaking color," Sharp World, [http://www.sharp-world.com/aquos/en/product/4\\_color\\_innovation.html#wrapper](http://www.sharp-world.com/aquos/en/product/4_color_innovation.html#wrapper) (23 November 2016).
- R. Soniera, "Display myths: shattered," Maximum PC, [http://www.displaymate.com/Display\\_Myths\\_Shattered.pdf](http://www.displaymate.com/Display_Myths_Shattered.pdf) (16 January 2017).
- D. L. MacAdam, "Projective transformations of I.C.I. color specifications," *J. Opt. Soc. Am.* **27**, 294 (1937).

**Sinan Genc** is a research assistant at Abdullah Gül University, Turkey. He received his BSc and MSc degrees in electrical electronics engineering from Sakarya University and electrical and computer engineering from Abdullah Gül University, respectively, and his current research interests include design and application of nanoplasmonics structures for new generation optoelectronic devices. He continues his PhD research in Mutlugun Research Laboratory in Abdullah Gül University.

**Mustafa Uguz** received his BSc and MSc degrees from METU, electrical and electronics engineering department, Turkey, in 2003 and 2006, respectively. Since 2004, he has been with Arçelik electronics plant research and development center, as a hardware design engineer, project manager and electronics plant research and development center responsible and coordinator, respectively. He managed several research programs and product development projects in academia and the private sector, funded by the Turkish State Agencies, TUBITAK, EU H2020, and industry.

**Osman Yilmaz** received his BSc degree in electrical and electronic engineering from Gazi University in 2003. He worked in the telecommunication area for two years at Atel Telekom, the electronics application area for two years at BekoElektronik A.Ş., and as a design engineer at Grundig Elektronik A.Ş. for seven years. He received an MBA degree from Koç University in 2015 and he has been working in the optical engineering area at Arçelik A.Ş.

**Evren Mutlugun** received his BSc degree from METU (2005) and MSc (2007) and PhD degrees (2011) in physics from Bilkent University. He worked as a research fellow at NTU, Singapore, between 2012 and 2014. His research focuses on quantum dot-based exciton harvesting systems. Currently, he is an associate professor at Abdullah Gul University, Turkey, and has coauthored numerous conference papers and more than 40 SCI journals of high rank in the field.